Cytotoxic Activity and DNA-Binding Investigations of Two Benzoxanthone Derivatives

Hui-Fang WANG,[a] Rui SHEN,[b] Lei JIA,[a] Jin-Cai WU,[a] and Ning TANG*,[a]

[a] College of Chemistry and Chemical Engineering, State Key Laboratory of Applied Organic Chemistry, Lanzhou University; Lanzhou 730000, P. R. China: and [b] College of Pharmacy, Nankai University; Tianjin 300071, P. R. China.
Received January 12, 2009; accepted May 8, 2009; published online May 11, 2009

In this study, the interactions of two benzoxanthones 1,3-dihydroxy-12*H*-benzo[*b*]xanthen-12-one (1) and 9,11-dihydroxy-12*H*-benzo[*a*]xanthen-12-one (2) with calf thymus DNA (ct DNA) have been investigated by absorption spectroscopy, fluorescence spectroscopy, circular dichroism spectroscopy and viscosity measurements. Experimental results suggested an intercalative mode with DNA for the two compounds; Furthermore, the binding affinity with DNA of 1 bearing linearly fused aromatic rings was higher than that of 2 bearing angularly fused aromatic rings according to the calculated binding constant values. In addition, three cell lines, the human cervical cancer cell line (HeLa), human hepatocellular liver carcinoma cell line (HepG2) and human normal liver cell line (L02) were used to evaluate the cytotoxic activities of the two benzoxanthones *in vitro*. As the results, they showed significant cytotoxic activity against the tumor cell lines HeLa and HepG2, but weak cytotoxic activity against normal liver cell line L02.

Key words benzoxanthone; DNA-binding; intercalative mode; cytotoxic activity

Natural products play a major role in anticancer drug discovery as a unique source of original structures which can provide models for future drug design. Xanthone compounds, secondary metabolites from higher plants and microorganisms, have very diverse biological profiles including anti-hypertensive, anti-oxidative, anti-thrombotic, and anticancer activity, based on their diverse structures.[1—7] During the past several years, the xanthone template has generated a growing interest in the search for new antitumor agents.[8] The preliminary work has highlighted the high potentials of xanthones as a promising building motif for the development of a new class of potent anticancer drugs.

Numerous biological experiments have demonstrated that DNA is one of the primary intracellular targets of anti-cancer drugs due to the interaction of small molecules with DNA, which cause DNA damage in cancer cells, block the division of cancer cells and result in cell death.[9] Up to now, few systematic studies of the interaction of xanthones and their derivatives with DNA have been reported.[10—12] However, their structure–activity relationships remain unestablished in the xanthones system. Benzoxanthones having four extended and conjugated fused rings may be viewed as flavone derivatives in which the phenyl group is fused with two aromatic rings. The structural features inherent in benzoxanthones, makes us aware that the conjugated π-systems in benzoxanthones may contribute significantly to the biological activity. The primary aim of this work was to gain some insight into the effect of structural factor in benzoxanthones on the probable binding mode and binding affinity toward DNA.

In this work, the binding mode on the interactions of two benzoxanthones 1,3-dihydroxy-12*H*-benzo[*b*]xanthen-12-one (**1**) and 9,11-dihydroxy-12*H*-benzo[*a*]xanthen-12-one (**2**) (shown in Fig. 1) with DNA was investigated by different kinds of spectrophotometric methods and viscosity measurements. The studies suggest that intercalative binding mode appears to be acceptable. In addition, the benzoxanthones were evaluated for cytotoxic activities toward human cervical cancer cell line (HeLa), human hepatocellular liver carcinoma cell (HepG2) and human normal liver cell line (L02) by acid phosphatase assay.

Experimental

Materials The benzoxanthones **1** and **2** were prepared according to the literatures[13—15] with some improvement. Calf thymus DNA (ct DNA) and ethidium bromide (EB) were obtained from Sigma Chemical Co. All the measurements were carried out in doubly distilled water buffer containing 5 mM Tris and 50 mM NaCl, and adjusted to pH 7.4 with hydrochloric acid. The concentration of DNA solution was determined from UV absorption at 260 nm using a molar absorption coefficient $\varepsilon_{260}=6600\,\mathrm{mol^{-1}\,cm^{-1}}$. Purity of the DNA was checked by monitoring the ratio of the absorbance at 260 nm to that at 280 nm. The solution gave a ratio of $A_{260}/A_{280}>1.80$, indicating that DNA was sufficiently free from protein.[16,17]

Physical Measurements The UV–Vis absorption measurements were conducted by using a Varian Cary 100 spectrophotometer equipped with quartz cells. All fluorescence emission spectra were measured using a Hitachi F-4500 spectrofluorophotometer equipped with a xenon lamp source and a quartz cell of 1 cm path length. Viscosity experiments were carried out on an Ubbelodhe viscometer. The circular dichroism (CD) spectra were recorded on a Jasco J-810 spectropolarimeter.

Methods Absorption titration experiments were performed by fixing concentrations of **1** and **2** as constant at 10 μM while varying the concentration of ct DNA. The absorption spectra changes of DNA were studied by fixing concentrations of DNA as constant at 100 μM while varying the concentration of **1** and **2**.

Fluorescence spectra of the competitive binding experiments were carried out by maintaining the EB and ct DNA concentration at 3 μM and 30 μM, respectively, while increasing the concentrations of the compounds. Fitting was completed using an Origin 6.0 spreadsheet, where values of the binding constants K_b were calculated.

Viscosity experiments were carried out on an Ubbelodhe viscometer, immersed in a thermostated water-bath maintained at 25.0±0.1 °C. Titrations were performed for the compounds (1—6 μM), and each compound was introduced into DNA solution (50 μM) present in the viscometer. Flow time was measured with a digital stopwatch and each sample was measured three times and an average flow time was calculated. Data were presented as

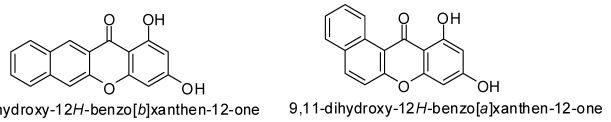

1,3-dihydroxy-12*H*-benzo[*b*]xanthen-12-one **1**

9,11-dihydroxy-12*H*-benzo[*a*]xanthen-12-one **2**

Fig. 1. The Structures of Benzoxanthones **1** and **2**

* To whom correspondence should be addressed. e-mail: tangn@lzu.edu.cn

$(\eta/\eta_0)^{1/3}$ *versus* the ratio of the concentration of the compound and DNA, where η is the viscosity of DNA in the presence of compound, and η_0 is the viscosity of DNA alone. Viscosity values were calculated from the observed flow time of DNA-containing solution corrected from the flow time of buffer alone (t_0), $\eta=t-t_0$.[18,19]

The CD spectra of DNA were recorded on a Jasco J-810 spectropolarimeter at 25.0±0.1 °C. Calf thymus DNA used were 200 μM in concentration and compounds solutions was added to a ratio of 1 : 1 (DNA/compound). Each sample solution was scanned in the range of 200—350 nm. CD spectrum was generated which represented the average of three scans from which the buffer background had been subtracted.

Acid Phosphatase Assay The reagent, *p*-nitrophenyl phosphate (*p*-NPP), was obtained from Amresco. The compounds synthesized were dissolved in dimethyl sulphoxide (DMSO) and diluted in culture medium. The final concentration of DMSO in cultures was always not exceeding 0.5% (v/v), which did not cause toxicity. The HeLa, HepG2 and L02 cells obtained from ATCC were maintained in Dulbecco's modified Eagle's medium (DMEM medium) with 10% FBS, 100 U/ml penicillin and 100 mg/ml streptomycin. Cells were cultured at 37 °C in a humidified atmosphere of 5% CO_2 in air.

Three different cell lines, uterine cervix carcinoma cell (HeLa), human hepatocellular liver carcinoma cell (HepG2) and human liver cell (L02) were plated in 96-well plates. The adherent cells, HeLa, HepG2 and L02 were plated at a density of 5×10^4 cells/ml, and then treated with varied concentration (10, 50, 100, 200, 300 μM) of the compounds. The culture medium was removed from the plates after 24, 48 and 72 h of culture, and each well was washed once with 200 μl phosphate-buffered saline (PBS, pH=7.2). To each well, 100 μl of buffer containing 0.1 M sodium acetate (pH=5.0), 0.1% Triton X-100, and 5 mM *p*-NPP was added. The reaction was stopped with the addition of 10 μl of 1 M NaOH, and color development was assayed at 405 nm using a microplate reader (Victor^3 1420-050). The nonenzymatic hydrolysis of the *p*-NPP substrate was determined for each assay by including wells that did not contain cells as blank wells. Cell survival was expressed as an absorbance (A) percentage defined by ($A_{\text{drug-blank}}/A_{\text{control-blank}}\times100$).

Results and Discussion

Electronic Absorption Spectra Electronic absorption spectroscopy is universally employed to examine the binding mode of DNA with small molecules. The absorption spectra of **1** and **2** in the absence and presence of ct DNA are given in Figs. 2a and b. In the absence of ct DNA, the UV–Vis absorption spectra of the benzoxanthone **1** has a strong π–π* transitions band at $\lambda_{max}=261$ nm and a strong n–π* transitions band at $\lambda_{max}=369$ nm, while the benzoxanthone **2** has a strong π–π* transitions band at $\lambda_{max}=208$ nm, a middle π–π* transition at $\lambda_{max}=266$ nm and a weak n–π* transitions band at $\lambda_{max}=328$ nm. With increasing DNA concentration, the absorption bands of the two compounds show decreases in molar absorptivity (hypochromism) as well as slight bathochromism. These variations are strongly indicative of the intercalation mode of the compounds with ct DNA, involving a strong π-stacking interaction between the compounds and DNA base pairs.[20,21]

In order to study the binding ability of the compounds with DNA quantitatively, the binding constant K_b was determined using the Eq. 1,[22]

$$[DNA]/(\varepsilon_a-\varepsilon_f)=[DNA]/(\varepsilon_b-\varepsilon_f)+1/K_b(\varepsilon_b-\varepsilon_f) \quad (1)$$

where [DNA] is the concentration of DNA in base pairs, ε_a, ε_f, and ε_b are the apparent extinction coefficient corresponding to A_{obsd}/[M], the extinction coefficient for the free compound and the extinction coefficient for the compound in the fully bound form, respectively. In plots of $[DNA]/(\varepsilon_a-\varepsilon_f)$ *versus* [DNA], K_b is given by the ratio of slope to the intercept (Figs. 2a, b, inset). The binding constants K_b for **1** and **2**

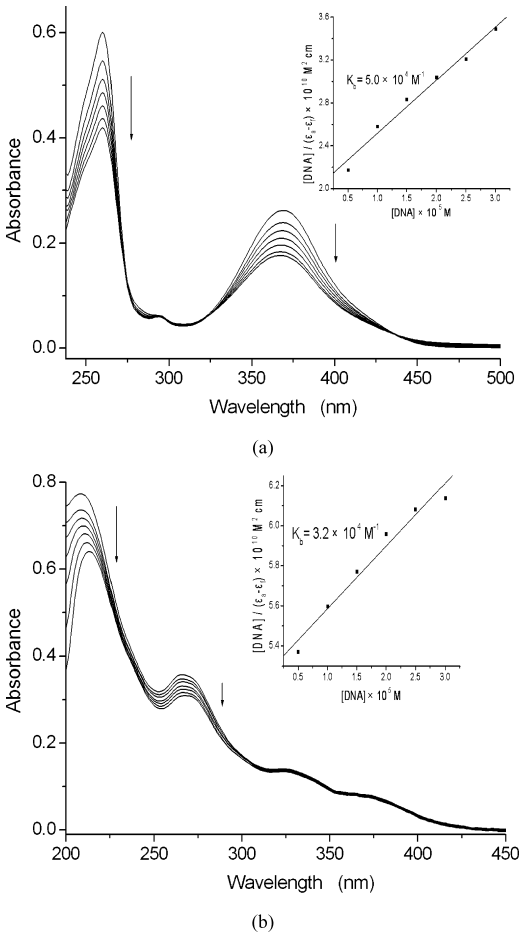

Fig. 2. UV–Vis Absorption Spectra of **1** (a) and **2** (b) (10 μM) in the Presence of 0, 5, 10, 15, 20, 25, 30 μM of ct DNA

The arrow indicates the absorbance changes upon increasing DNA concentration. The inset is plot of $[DNA]/(\varepsilon_b-\varepsilon_f)$ *vs.* [DNA] for the titration of DNA to the compounds.

were found to be 5.0×10^4 M^{-1} and 3.2×10^4 M^{-1}, respectively. The results indicate that the binding strength of compound **1** is stronger than **2**. Because there are absorption bands at about 260 nm for the two benzoxanthones and DNA, the binding constants K_b were obtained from extinction coefficients of other absorbance bands at $\lambda_{max}=369$ nm and $\lambda_{max}=208$ nm for **1** and **2**, respectively.

Furthermore, the spectra changes process of DNA could indicate the corresponding changes of DNA in its conformation and structure after the small molecule bonds to DNA *via* various noncovalent interactions.[23,24] Hyperchromic or hypochromic effect is the spectra features of DNA concerning its double helix structure. Hyperchromism results from the damage of the DNA double helix structure, while hypochromism results from the contraction of DNA in the helix axis, as well as from the change in conformation on DNA. Figures 3a and b both display a well-behaved titration of **1** and **2** with calf thymus DNA. With increasing concentration of the compounds, the absorption intensity at 260 nm of DNA exhibit visible hyperchromism of about 46.67% and 24.29% for **1** and **2**, respectively. This phenomenon may have been largely due to the fact that the purine bases and pyrimidine bases of DNA were exposed because of the interaction of the benzoxanthones to DNA.[25] So this typical hyper-

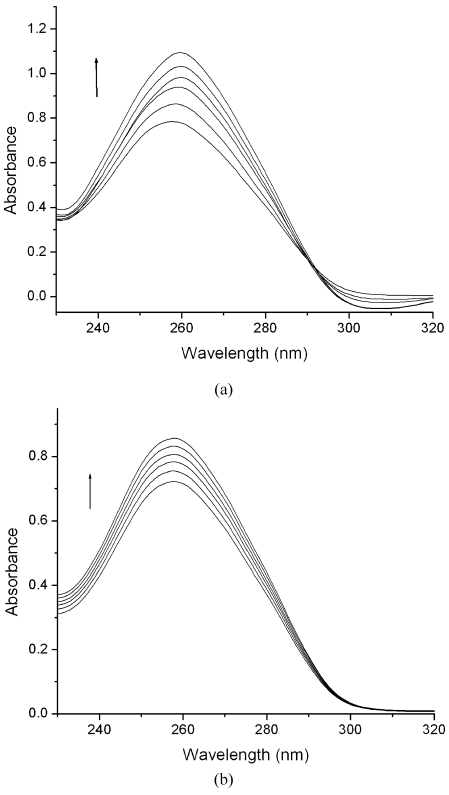

Fig. 3. UV–Vis Absorption Spectra of ct DNA in the Presence of 0, 10, 20, 30, 40, 50 μM of **1** (a) and **2** (b)

[DNA]=100 μM.

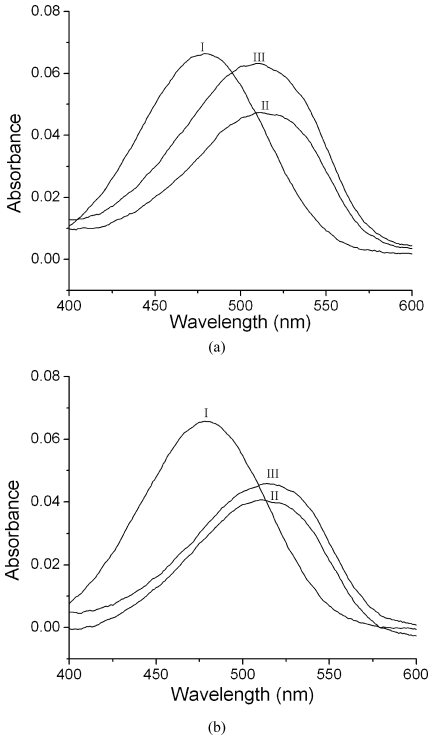

Fig. 4. The Visible Absorption Spectra of (a) 10 μM EB (I); 10 μM EB+10 μM DNA (II); 10 μM EB+10 μM DNA+10 μM **1** (III) and (b) 10 μM EB (I); 10 μM EB+10 μM DNA (II); 10 μM EB+10 μM DNA+10 μM **2** (III)

chromic effect also confirms the interaction of compounds to DNA evidenced by the changes of the DNA double helix structure after the benzoxanthones bound to DNA.[26)]

In order to confirm the binding mode of DNA with the two benzoxanthones, ethidium bromide (EB) was employed in this experiment, as EB interacts presumably with DNA as a typical indicator of intercalation. Figures 4a and b show that the maximal absorption of EB at 479 nm decreased and shifted to 511 nm in the presence of DNA, which is characteristic of intercalation. As shown in Figs. 4a and b, curve III is the absorption of the mixture solution of EB, the compounds and DNA. It is found that the absorption at 511 nm increased comparing with curve II, which indicates there existing competitive intercalation between the compounds and EB with DNA.[27)] Furthermore, the increased extent of the absorption when addition **1** is more apparent than addition compound **2**, which may reflect the relative DNA-binding affinities of **1** and **2**.

Fluorescence Spectra EB has characteristics of high sensitivity and selectivity to DNA. Fluorescence intensity of EB is so weak, but the intensity greatly increases when EB intercalated into DNA. It was previously reported that the enhanced fluorescence could be quenched, at least partially, by addition of a second intercalative molecule.[28,29)] The quenching extents of fluorescence of EB bound to DNA are used to determine the relative DNA-binding affinities of the second molecules.

Therefore, the binding mode of DNA with **1** and **2** also can be checked by competitive binding experiment. The emission spectra of DNA–EB system in the presence of increasing amounts of **1** and **2** are shown in Figs. 5a and b respectively. It can be noted that intensity of the fluorescence spectrum at 587 nm decreased apparently by addition of increasing amounts of the two compounds, which confirms that both of them interact with DNA by an intercalating mechanism, competing with EB for the same binding sites. The result was caused by EB changing from a hydrophobic environment to an aqueous environment.[30,31)]

According to the classical Stern–Volmer equation, Eq. 2[32)]:

$$F_0/F = 1 + K_q[Q] \quad (2)$$

Where F_0 and F represent the emission intensity in the absence and presence of quencher, respectively, K_q is a linear Stern–Volmer quenching constant and [Q] is the quencher concentration. The quenching plots illustrate that the quenching of EB bound to DNA by the compounds is in good agreement with (R=0.99) the linear Stern–Volmer equation (Figs. 5a and b, inset). In the plots of F_0/F *versus* [Q], K_q is given by the ratio of the slope to the intercept. The K_q value for **1** is $1.3\times10^5\,M^{-1}$ while the compound **2** is $7.4\times10^4\,M^{-1}$, which shows that **1** is more able than **2** in replacing the strong DNA intercalators EB, in consistent with the higher value of K_b spectrophotometrically determined. This result is in accordance with DNA intercalation mechanism for both benzoxanthones, being **1** characterized by higher affinity toward DNA, compared with **2**.

CD Spectroscopy Circular dichroic spectral techniques may give us useful information on how the conformation of the DNA chain is influenced by small molecules. The CD spectrum of ct DNA consists of a positive band at 275 nm that can be due to base stacking and a negative band at

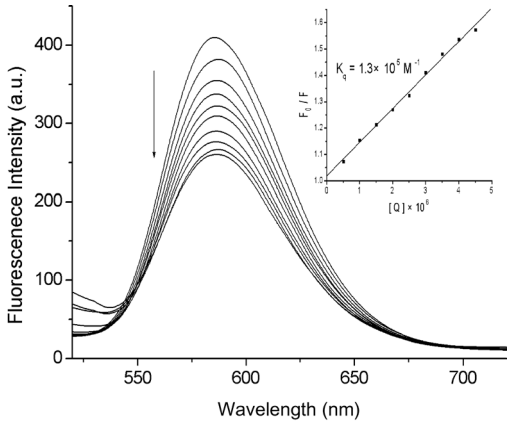

(a)

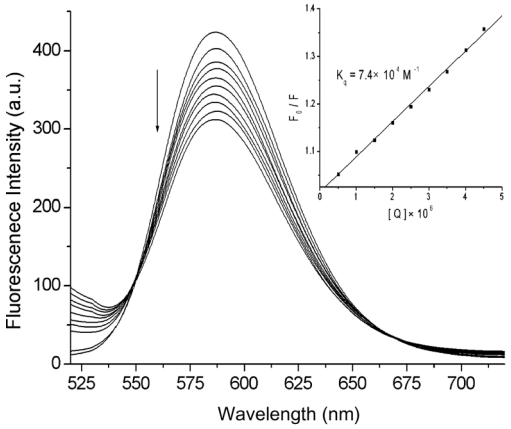

(b)

Fig. 5. Fluorescence Emission Spectra of DNA–EB in the Presence of 0, 0.5, 1, 1.5, 2, 2.5, 3, 3.5, 4, 4.5 μM of **1** (a) and **2** (b)

λ_{ex}=500 nm, λ_{em}=520—720 nm. Arrow shows the emission intensities upon increasing compounds concentration. The inset is Stern–Volmer quenching plots of the fluorescence titration.

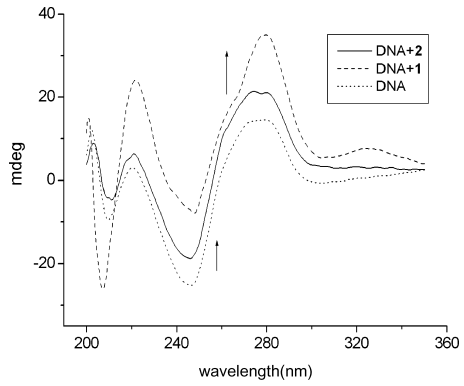

Fig. 6. CD Spectra of ct DNA (200 μM) in the Absence and Presence of **1** (200 μM) and **2** (200 μM)

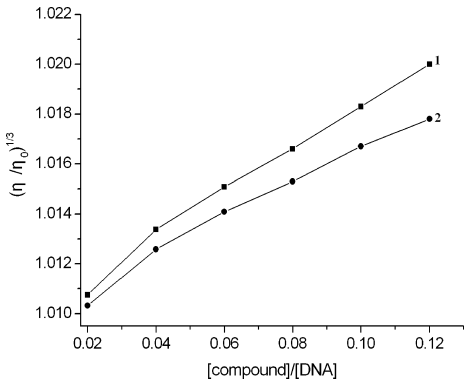

Fig. 7. Effect of Increasing Amounts of the Compounds **1** (Line 1) and **2** (Line 2) on the Relative Viscosity of ct DNA at 25 °C

[DNA]=50 μM, [compound]=1, 2, 3, 4, 5, 6 μM.

245 nm that can be due to helicity and it is also characteristic of DNA in a right-handed B form.[33] The changes in CD signals of DNA observed on interaction with small molecules may often be assigned to the corresponding changes in DNA structure.[34] Thus simple groove binding and electrostatic interaction of small molecules show less or no perturbation on the base-stacking and helicity bands, whereas intercalation enhances the intensities of both the bands stabilizing the right-handed B conformation of ct DNA as observed for the classical intercalators methylene blue.[35]

The CD spectrum of ct DNA was monitored in the presence of **1** and **2**; the changes observed in the two cases are shown in Fig. 6. On addition of **2** to ct DNA, it shows slight red shift with intensity increase and decrease in the positive and negative bands respectively. When addition of compound **1** to ct DNA, it is observed that the positive-band position was shifted to 280 nm from 275 nm with more evident increase than **2** in molar ellipticity, while the intensity of the negative band in the CD spectrum of DNA was perturbed with a red shift of 3 nm. This reveals the effect of strong intercalation of the compounds on base stacking and decreased right-handedness of B-DNA. Furthermore, the large decrease in intensity of the DNA helicity band indicates that the DNA is unwound upon interaction with the compounds and then transformed into other conformations.[36—38] The result is in agreement with structure changes concluded from absorbance spectra changes process of DNA upon adding the two compounds.

Viscosity Studies Optical photophysical probes generally provide necessary, but not sufficient clues to support a binding mode. Hydrodynamic measurements that are sensitive to length change (*i.e.,* viscosity and sedimentation) are regarded as the least ambiguous and the most critical tests of binding in solution in the absence of crystallographic structural data. A classical intercalation model results in lengthening the DNA helix as base pairs are separated to accommodate the binding small molecules, leading to an increase of DNA viscosity. In contrast, a partial and non-classical intercalation of small molecules could bend or kink the DNA helix, reduce its effective length and increase its viscosity concomitantly.[39]

As a validation of the above verdict, viscosity measurements were carried out. The effects of the two compounds on the viscosity of DNA at 25.0±0.1 °C are shown in Fig. 7. It can be observed that the viscosity of the DNA increased with increasing amounts of **1** or **2**. Such behavior is in accordance with other intercalators, which increases the relative specific viscosity for the lengthening of the DNA double helix resulting from intercalation. These results indicate that the two compounds can intercalate between adjacent DNA base pairs, causing an extension in the helix, and thus increase the viscosity of DNA. **1** can intercalate more deeply than **2**. The results obtained from viscosity studies also validate those ob-

Table 1. Antiproliferative Effects (IC_{50}) of **1** and **2** on HeLa Cells, HepG2 Cells and L02 Cells

Compound	HeLa cells (μM)			HepG2 cells (μM)			L02 cells (μM)		
	24 h	48 h	72 h	24 h	48 h	72 h	24 h	48 h	72 h
1	>300	41.5	8.3	>300	255	92	>300	>300	152
2	>300	49.6	24.4	>300	36.5	41	>300	>300	>300

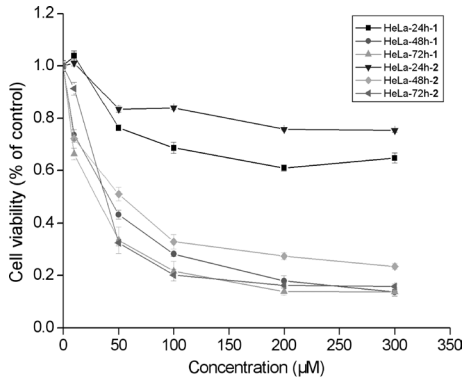

(a)

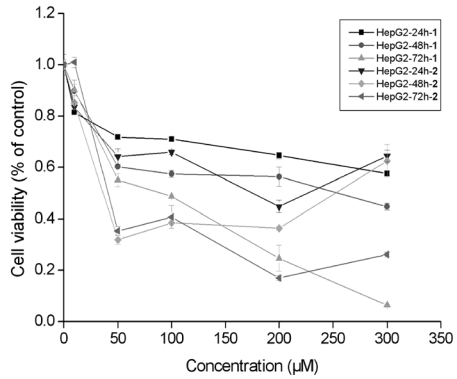

(b)

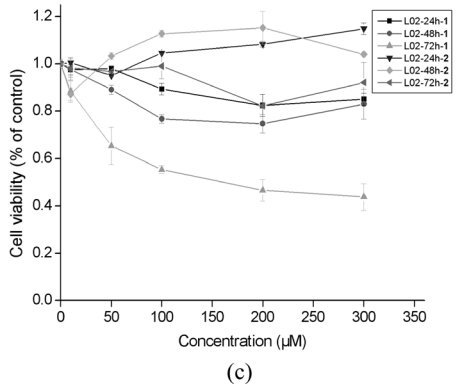

(c)

Fig. 8. Effects of **1** and **2** on Viability of HeLa (a), HepG2 (b) and L02 (c) Cells

Cells were treated with various concentrations of **1** and **2** for indicated duration. Each data point represents the arithmetic mean±S.D. of three independent experiments.

tained from the spectroscopic studies. On the basis of all the spectroscopic studies together with the viscosity measurements, it is suggested that the two benzoxanthones **1** and **2** could bind to ct DNA in non-classical intercalation mode.

Cytotoxic Activities To evaluate the potential antiproliferative activity of the compounds, human cervical cancer cell line (HeLa), human hepatocellular liver carcinoma cell line (HepG2) and human normal liver cell line (L02) were incubated for 24 h, 48 h and 72 h with varying concentrations of them and the cell viability was determined by acid phosphatase assay. The assay is based on the hydrolysis of the *p*-nitrophenyl phosphate by intracellular acid phosphatases in viable cells to produce *p*-nitrophenol. For the cell lines examined, absorbance of *p*-nitrophenol at 405 nm is directly proportional to the cell number in the range of 10^3—10^5 cells.

The cell viability was decreased in response to **1** and **2** in a dose-dependent manner as illustrated in Fig. 8 and Table 1. The compounds didn't show evident cytotoxic activity against tumor cell lines HeLa and HepG2 when treatment with 24 h. However, they showed potent cytotoxic activity against them after 48 h and 72 h treatment. They exhibited very weak cytotoxic activity against L02 except for **1** when treatment for 72 h. The results demonstrated that the tumor cell line HeLa and HepG2 were more susceptible to the two benzoxanthones as compared with that of normal cell line L02. It may be because the compounds induce damage to DNA in the cancer cells.[9]

The compound **1** bearing linearly fused aromatic ring had more potent activity than **2** bearing angularly fused aromatic ring against HeLa, while **2** had more preferable activity toward HepG2 comparing to **1**. It reveals that the cytotoxic activity of the same compound against one tumor cell line differs from another. This suggests that the action mechanisms of benzoxanthones against HeLa may be different from that against HepG2. It may be due to the different structures and compositions in various tumor cell lines. The complicated mechanisms about the effect of the compounds on the tumor cells are currently under the way.

Conclusion

The interaction mode between DNA and the two benzoxanthones have been investigated by spectrophotometric methods and viscosity measurements. The results suggest that the two compounds can intercalate into the base group pairs of DNA because of the good planarity of the benzoxanthone ring. They both have strong binding affinity with DNA. Comparing the binding extents of them, it is concluded that binding affinity of **1** bearing linearly fused aromatic ring is stronger than **2** bearing angularly fused aromatic rings. Moreover, the result of acid phosphatase assay suggested that they had potent cytotoxic activity against tumor cell lines HeLa and HepG2 but weak effect on normal liver cell line L02.

Acknowledgement We are grateful for the financial support of the National Science Foundation of China (20601011).

References

1) Pinto M. M. M., Sousa M. E., Nascimento M. S., *J. Curr. Med. Chem.*, **12**, 2517—2538 (2005).

2) Peres V., Nagem T. J., Oliveira F. F. D., *Phytochemistry*, **55**, 683—710 (2000).
3) Jung H. A., Su B. N., Keller W. J., Mehta R. G., Kinghorn A. D., *J. Agric. Food Chem.*, **54**, 2077—2082 (2006).
4) Lee B. W., Lee J. H., Lee S. T., Lee H. S., Lee W. S., Jeong T. S., Park K. H., *Bioorg. Med. Chem. Lett.*, **15**, 5548—5552 (2005).
5) Lembège M. V., Moreau S., Larrouture S., Montaudon D., Robert J., Nuhrich A., *Eur. J. Med. Chem.*, **43**, 1336—1343 (2008).
6) Yoshimi N., Matsunaga K., Katayama M., Yamada Y., Kuno T., Qiao Z., Hara A. J., Mori H., *Cancer Lett.*, **163**, 163—170 (2001).
7) Sanugul K., Akao T., Li Y., Kakiuchi N., Nakamura N., Hattori M., *Biol. Pharm. Bull.*, **28**, 1672—1678 (2005).
8) Sittisombut C., Costes N., Michel S., Kochm M., Tillequin F., Pfeiffer B., Renard P., Pidrrè A., Atassi G., *Chem. Pharm. Bull.*, **49**, 791—793 (2001).
9) Zuber G., Quada J. C. J., Hecht S. M., *J. Am. Chem. Soc.*, **120**, 9368—9369 (1998).
10) Pace T. C. S., Monahan S. L., MacRae A. I., Kaila M., Bohne C., *Photochem. Photobiol.*, **82**, 78—87 (2006).
11) Adam S. J., Lajos Z. S., Mary C. G. G., Laurence H. H., *J. Med. Chem.*, **48**, 2993—3004 (2005).
12) Hansen M., Lee S. J., Cassady J. M., Hurley L. H., *J. Am. Chem. Soc.*, **118**, 5553—5561 (1996).
13) Sittisombut C., Boutefnouchet S., Vanduft H. T., Tian W., Michel S., Koch M., Tillequin F., Pfeiffer B., Pidrre A., *Chem. Pharm. Bull.*, **54**, 1113—1118 (2006).
14) Liu Y., Ma L., Chen W. H., Wang B., Xu Z. L., *Bioorg. Med. Chem.*, **15**, 2810—2814 (2007).
15) Liu Y., Ke Z. F., Cui J. F., Chen W. H., Ma L., Wang B., *Bioorg. Med. Chem.*, **16**, 7185—7192 (2008).
16) Huang C. Z., Li Y. F., Feng P., *Talanta*, **55**, 321—328 (2001).
17) Kumar C. V., Asuncion E. H., *J. Am. Chem. Soc.*, **115**, 8547—8553 (1993).
18) Eriksson M., Leijon M., Hiort C., Norden B., Gradslund A., *Biochemistry*, **33**, 5031—5040 (1994).
19) Xiong Y., He X. F., Zou X. H., Wu J. Z., Chen X. M., Ji L. N., Li R. H., Zhou J. Y., Yu K. B., *J. Chem. Soc. Dalton Trans.*, **1999**, 19—24 (1999).
20) Kelly J. M., Murphy M. J., Mcconnell D. J., Ohuigin C., *Nucleic Acids Res.*, **13**, 167—184 (1985).
21) Bloomfield V. A., Crothers D. M., Tinico I. J. I., "Physical Chemistry of Nucleic Acids," Harper and Row, New York, 1974, pp. 429—476.
22) Mudasir, Yoshioka N., Inoue H., *J. Inorg. Biochem.*, **77**, 239—247 (1999).
23) Zhou C. Y., Zhao J., Wu Y. B., Yin C. X., Yang P., *J. Inorg. Biochem.*, **101**, 10—18 (2007).
24) Zhou Q. H., Yang P., *Inorg. Chim. Acta*, **359**, 1200—1206 (2006).
25) Song Y. M., Wu Q., Yang P. J., Luan N. N., Wang L. F., Liu Y. M., *J. Inorg. Biochem.*, **100**, 1685—1691 (2006).
26) Carter M. T., Allen J., *J. Am. Chem. Soc.*, **109**, 7528—7530 (1987).
27) Boger D. L., Fink B. E., Brunette S. R., Tse W. C., Hedrick M. P., *J. Am. Chem. Soc.*, **123**, 5878—5891 (2001).
28) Lippard S. J., *Acc. Chem. Res.*, **11**, 211—217 (1978).
29) Lepecq J. B., Paoletti C., *J. Mol. Biol.*, **27**, 87—106 (1967).
30) Zeng Y. B., Yang N., Liu W. S., Tang N., *J. Inorg. Biochem.*, **97**, 258—264 (2003).
31) Kumar C. V., Barton J. K., Turro N. J., *J. Am. Chem. Soc.*, **107**, 5518—5523 (1985).
32) Efink M. R., Ghiron C. A., *Anal. Biochem.*, **114**, 199—227 (1981).
33) Ivanov V. I., Minchenkova L. E., Schyolkina A. K., Poletayer A. I., *Biopolymers*, **12**, 89—110 (1973).
34) Lincoln P., Tuite E., Norden B., *J. Am. Chem. Soc.*, **119**, 1454—1455 (1997).
35) Norden B., Tjerneld F., *Biopolymers*, **21**, 1713—1734 (1982).
36) Vaidyanathan V. G., Vijayalakshmi R., Subramanain V., Nair B. U., *Bull. Chem. Soc. Jpn.*, **75**, 1143—1149 (2002).
37) Chauhan M., Arjmand F., *Chem. Biodiversity*, **3**, 660—676 (2006).
38) Maheswari P. U., Palaniandavar M., *J. Inorg. Biochem.*, **98**, 219—230 (2004).
39) Zou X. H., Ye B. H., Li H., Liu J. G., Xiong Y., Ji L. N., *J. Chem. Soc. Dalton Trans.*, **1999**, 1423—1428 (1999).